J Biomol NMR (2014) 59:263–277
DOI 10.1007/s10858-014-9845-z

ARTICLE

Cryoprotection of lipid membranes for high-resolution solid-state NMR studies of membrane peptides and proteins at low temperature

Myungwoon Lee · Mei Hong

Received: 2 June 2014 / Accepted: 3 July 2014 / Published online: 12 July 2014

Abstract Solid-state NMR spectra of membrane proteins often show significant line broadening at cryogenic temperatures. Here we investigate the effects of several cryoprotectants to preserve the spectral resolution of lipid membranes and membrane peptides at temperatures down to ~200 K. Trehalose, glycerol, dimethylsulfoxide (DMSO), dimethylformamide (DMF), and polyethylene glycol (PEG), were chosen. These compounds are commonly used in protein crystallography and cryobiology. ^{13}C and ^{1}H magic-angle-spinning spectra of several types of lipid membranes show that DMSO provides the best resolution enhancement over unprotected membranes and also best retards ice formation at low temperature. DMF and PEG-400 show slightly weaker cryoprotection, while glycerol and trehalose neither prevent membrane line broadening nor prevent ice formation under the conditions of our study. Neutral saturated-chain phospholipids are the most amenable to cryoprotection, whereas negatively charged and unsaturated lipids attenuate cryoprotection. ^{13}C–^{1}H dipolar couplings and ^{31}P chemical shift anisotropies indicate that high spectral resolution at low temperature is correlated with stronger immobilization of the lipids at high temperature, indicating that line narrowing results from reduction of the conformational space sampled by the lipid molecules at high temperature. DMSO selectively narrowed the linewidths of the most disordered residues in the influenza M2 transmembrane peptide, while residues that exhibit narrow linewidths in the unprotected membrane are less impacted. A relatively rigid β-hairpin antimicrobial peptide, PG-1, showed a linewidth increase of ~0.5 ppm over a ~70 K temperature drop both with and without cryoprotection. Finally, a short-chain saturated lipid, DLPE, exhibits excellent linewidths, suggesting that it may be a good medium for membrane protein structure determination. The three best cryoprotectants found in this work—DMSO, PEG, and DMF—should be useful for low-temperature membrane-protein structural studies by SSNMR without compromising spectral resolution.

Keywords Cryoprotection · Linewidth · Dimethylsulfoxide · Polyethylene glycol · Glycerol · Conformational disorder

Introduction

Magic-angle-spinning (MAS) solid-state NMR (SSNMR) spectroscopy is a powerful technique for determining the high-resolution structures of membranes proteins (Cady et al. 2010; Lange et al. 2006), amyloid fibrils (Tang et al. 2013; Tycko 2011; Wasmer et al. 2008), and other biological systems such as bacterial and plant cell walls (Dick-Perez et al. 2011; Loquet et al. 2012; Renault et al. 2012; Wang et al. 2013a, b). For most non-crystalline compounds, the linewidths of SSNMR spectra are much larger than solution NMR spectra of soluble molecules, even when fast MAS, strong ^{1}H decoupling, and ^{1}H dilution are employed, because a major source of the linewidths, which cannot be remedied by radiofrequency pulses, is molecular conformational disorder, which creates a distribution of chemical shifts for each chemically inequivalent nuclear spin. At ambient temperature, molecular motions such as small-amplitude torsional fluctuations and sidechain

Electronic supplementary material The online version of this article (doi:10.1007/s10858-014-9845-z) contains supplementary material, which is available to authorized users.

M. Lee · M. Hong (✉)
Department of Chemistry, Iowa State University, Ames, IA 50011, USA
e-mail: meihong@mit.edu

reorientations are present to partially average this conformational distribution and narrow the chemical shift linewidths. But at low temperature, motions slow down sufficiently, thus broadening the linewidths to reflect the conformational and dynamic disorder at high temperature (Su et al. 2010; Su and Hong 2011).

Cryogenic-temperature SSNMR spectroscopy has become increasingly important in recent years due to the advent of high-frequency dynamic nuclear polarization (DNP) and studies of transient biological processes (Tycko 2013). DNP enhances the NMR sensitivity by as much as two orders of magnitude by transferring the electron polarization to nuclei (Carver and Slichter 1956; Maly et al. 2008; Ni et al. 2013) and is best conducted below ~100 K where the sensitivity enhancement is high. To study transient states during fast processes such as protein folding, these states need to be trapped by low temperature (Hu et al. 2010). However, at cryogenic temperatures, moderate to severe line broadening has been observed for many hydrated biological samples (Linden et al. 2011; Siemer et al. 2012), even when these samples are protected by a glycerol-water solution to minimize ice formation. Exceptions to this low-temperature line broadening have been reported for an anhydrous peptide crystal (Bajaj et al. 2009) and hydrated GB1 that contains high concentrations of a cryoprotectant (Franks et al. 2005).

If low-temperature line broadening significantly results from the trapping of multiple molecular conformations that are sampled at high temperature, then in principle one approach to minimize this line broadening is to reduce the high-temperature dynamic and conformational disorder, as long as the disorder is not functionally important. In this work, we investigate the utilities of several cryoprotectants for narrowing the linewidths of lipid membranes and membrane peptides at temperatures down to ~200 K. Cryoprotectants are commonly used in cell biology (Labbe et al. 1997; Storey et al. 1998), protein crystallography (Petsko 1975; Rosenbaum et al. 2011), and cryoelectron microscopy and tomography (Tivol et al. 2008) to preserve the structural and functional integrity of cells and macromolecules. However, comparisons of the efficacies of cryoprotectants have often led to contradicting results, and molecular insights are limited. It is known that the cryoprotecting effect on lipid membranes is only partly colligative; electrostatic interactions with lipid polar moieties and hydrophobic interactions with acyl chains are also involved. Importantly, the goals of cell cryobiology—preventing cell–cell fusion, preventing intracellular ice formation, retaining enzyme function, and avoiding chemical toxicity—do not fully align with the purpose of cryoprotection in structural biology, which is to preserve the structural homogeneity and avoid structural distortions of biomolecules at low temperature. For these reasons, it is important to examine how various cryoprotectants perform under typical SSNMR conditions for membrane protein structure determination.

In this study, we investigate the effects of five cryoprotectants—trehalose, glycerol, polyethylene glycol (PEG), dimethylsulfoxide (DMSO), and dimethylformamide (DMF) (Fig. 1)—on the ^{13}C, ^{1}H and ^{31}P MAS spectra of several lipid membranes and two membrane peptides. These cryoprotectants were chosen for their chemical diversity, since they represent the sugar, glycol, sulfoxide and amide families of cryoprotectants. The lipid ^{13}C linewidths were measured from 303 to 203 K, and the ^{1}H spectra were measured to monitor water dynamics. Temperatures much lower than 200 K are not accessed in the present study due to experimental limitations. Based on the 203 K spectral resolution, we find that the standard glycerol/water mixture is clearly inferior to the other cryoprotectants except for trehalose, while DMSO, DMF and PEG show significant resolution enhancement over the unprotected membranes. One of the best line-narrowing compounds, DMSO, strongly immobilizes the lipid polar region, supporting the hypothesis that reducing lipid dynamic disorder at high temperature leads to narrower linewidths at low temperature. DMSO enhanced the spectral resolution of the influenza M2 transmembrane peptide (M2TM), by reducing the linewidths of the most disordered residues. Finally, we show that DLPE is an unusually well-ordered lipid with high-resolution NMR spectra both with and without cryoprotectants, thus it is a promising medium for membrane-protein structure determination.

Materials and methods

Membrane sample preparation

Five lipid membranes were used in this study: 1,2-dimyristoyl-sn-glycero-3-phosphocholine (DMPC), 1,2-dioleoyl-*sn*-glycero-3-phosphocholine (DOPC), a 3:1 molar mixture of DOPC and 1,2-dioleoyl-*sn*-glycero-3-phosphoglycerol (DOPG), 1,2-dilauroyl-*sn*-glycero-3-phosphocholine (DLPC), and 1,2-dilauroyl-*sn*-glycero-3-phosphoethanolamine (DLPE). For single-component membranes, the lipids were directly suspended in pH 7.5 Tris buffer (10 mM Tris base, 1 mM EDTA, 0.1 mM NaN_3) and subjected to seven freeze–thaw cycles to create homogeneous vesicles. DLPE required 10 min of bath sonication and ten freeze–thaw cycles to produce a sufficiently homogeneous vesicle solution. For the DOPC/DOPG mixture, the two lipids were codissolved in chloroform, the solvent was dried under nitrogen gas, then the lipids were lyophilized overnight. The dry powder was then suspended in buffer to make the vesicle solution. Lipid vesicle solutions were centrifuged at 150,000*g* using a Beckman SW60Ti rotor at 277 K for

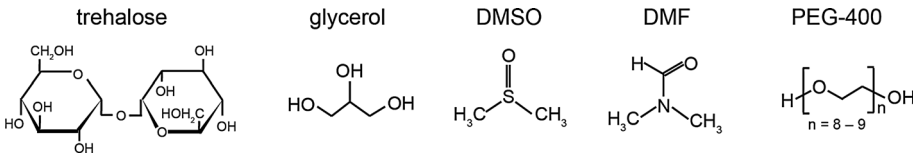

Fig. 1 Structures of the cryoprotectants used in this study

Table 1 Compositions of cryoprotected lipid membranes

Lipids (T_m in K)	Cryoprotectants	Lowest freezing point of water	Lipid:Cryoprotectant:Buffer amounts (mole ratio)
DMPC (296 K)	Trehalose	193 K (60 wt%)[a]	15 mg:10 mg:16 mg (1:1.2:40.2)
	Glycerol	226 K (67 wt%)[a]	15 mg:5.3 μL:5.3 μL (1:3.2:13.2)
	DMSO	203 K (70 wt%)[a]	15 mg:6 μL:6 μL (1:3.8:15.1)
	PEG-400	218 K (68 wt%)[a]	15 mg:6 μL:6 μL (1:0.8:15.1)
	DMF	188 K (82 wt%)[a]	15 mg:6 μL:3.8 μL (1:2.9:9.5)
DOPC (253 K)	DMSO		15 mg:7.5 μL:3.8 μL (1:5.5:11)
DLPC (272 K)	DMSO		15 mg:7.5 μL:3.8 μL (1:4.4:8.8)
DLPE (302 K)	DMSO		15 mg:8 μL:4 μL (1:4.4:8.6)
DOPC/DOPG (254 K)	DMSO		15 mg:8 μL:4 μL (1:5.9:11.7)
	DMF		15 mg:6 μL:6 μL (1:3.4:17.5)
	PEG 400		15 mg:8 μL:4 μL (1:1.2:11.7)

[a] Percentages are the mass of the cryoprotectant relative to the total cryoprotectant and water mass

4 h to obtain membrane pellets. The cryoprotectants, dissolved in Tris buffer, were titrated into the membrane pellets and the samples were vortexed and equilibrated at room temperature until the desired hydration level and stoichiometric ratios (Table 1) were reached. All cryoprotectants used here have much lower vapor pressures than water at ambient temperature, thus the slow dehydration process mostly removes excess water instead of the cryoprotectants. The equilibrated membranes were spun down into 4 mm MAS rotors using pipette tips.

Our method of titrating cryoprotectants directly to membrane pellets differs from the typical sample preparation method in cryobiology, where cryoprotectants are added in solution at concentrations of 0.1–1 M. Thus, those cell biology experiments do not directly control the extent of cryoprotectant binding to the membrane, and different cryoprotectants in general would bind the membrane to different extents due to their different partition coefficients.

We prepared a second trehalose-bound DMPC sample using a different protocol, by adding trehalose to the lipid vesicle solution before freeze–thaw cycles, then spinning down the membrane. This procedure tests whether we can maximize trehalose binding to lipid bilayers to give better cryoprotection, since the non-permeable trehalose may not bind uniformly to multilamellar vesicles obtained after pelleting.

A D44A mutant of M2TM (residues 22–46, SSDPLVVAASII GILHLILWILARL) was synthesized using Fmoc chemistry by PrimmBiotech (Cambridge, MA) and purified to >95 % purity. Uniformly ^{13}C, ^{15}N-labeled amino acids (Sigma-Aldrich and Cambridge Isotope Laboratories) were incorporated at residues L26, V27, S31, G34, and A44. The peptide was dissolved in octyl-β-D-glucoside (OG) and mixed with lipid vesicles, incubated at room temperature for ~3 h, then dialyzed against the pH 7.5 Tris buffer for 2 days with 2 buffer changes per day to remove OG. The dialyzed proteoliposome solution was centrifuged to obtain membrane pellets. The antimicrobial peptide, protegrin-1 (PG-1), was bound to DLPE vesicles directly in solution due to the high solubility of the peptide. The PG-1 sample contains isolated labels at Leu5 $^{13}C\alpha$, Val16 $^{13}C'$, and Phe12 ^{19}F. The peptide-bound vesicles were incubated at room temperature overnight before centrifugation. DMSO was directly titrated into the pellet to obtain the cryoprotected sample.

Solid-state NMR experiments

SSNMR spectra were measured on a Bruker DSX-400 MHz (9.4 T) spectrometer and an AVANCE 600 MHz (14.1 T) spectrometer using 4 mm MAS probes. 1D ^{1}H direct-polarization (DP) spectra and ^{13}C DP and cross-polarization (CP) spectra were measured from 303 to 203 K. The MAS frequency was typically 7 kHz. The samples were equilibrated for 30 min at each temperature before measurements. 1D ^{13}C double-quantum filtered (DQF) spectra for M2TM-containing membranes were measured under 8 kHz MAS using the SPC5 sequence for ^{13}C–^{13}C dipolar recoupling. 1D ^{31}P MAS spectra were measured at 5 kHz to obtain sideband intensities as an indicator of motionally averaged chemical shift anisotropy (CSA), which gives information on the lipid headgroup dynamics.

^{13}C-^{1}H dipolar couplings were measured using the 2D dipolar chemical-shift (DIPSHIFT) correlation experiment (Munowitz et al. 1981) under 3.3 kHz MAS at 280 K. For ^{1}H homonuclear decoupling, the MREV-8 sequence was used with a ^{1}H 105° pulse length of 3.5 μs. The t_1 dimension was fit to obtain the apparent dipolar coupling, which was divided by the theoretical MREV-8 scaling factor of 0.47 to obtain the true coupling. The C–H order parameter S_{CH} was calculated as the ratio of the true coupling to a rigid-limit value of 22.7 kHz. The model compound N-formyl-MLF (Hong and Griffin 1998; Rienstra et al. 2002) was used to verify the MREV-8 scaling factor.

Results

Effects of cryoprotectants on DMPC bilayers

To investigate whether cryoprotectants enhance the spectral resolution at low temperature compared to unprotected membranes, we measured the ^{13}C and ^{1}H spectra of lipid membranes bound to five cryoprotectants. The disaccharide trehalose is a non-permeable cryoprotectant while glycerol, DMSO, DMF, and PEG-400 are permeable, in the sense that they are able to cross the bilayer to suppress intracellular ice formation. In the ternary system formed by the lipid, cryoprotectant, and water, the cryoprotectant amount was 40–70 wt% relative to the lipid, and the total cryoprotectant plus water mass was ∼40 wt% of the total sample mass for most samples (Table 1). For the solid trehalose, more buffer was used to reach a hydration level of 40 wt%. These compositions were chosen based on two considerations. First, the phase diagrams of cryoprotectant/water solutions (Baudot and Boutron 1998; Huang and Nishinari 2001; Lane 1925; Miller et al.1997; Murata and Tanaka 2012; Rasmussen and MacKenzi 1968) place the minimum water freezing point at cryoprotectant concentrations of 60–80 wt% of the total cryoprotectant/water solution. Second, the cryoprotectant/lipid ratio should not be too high to disrupt the membrane nor too low to have no effect. All five cryoprotectants are fully miscible with water, thus we added them to the membrane pellets after centrifugation, to ensure that a sufficient amount of cryoprotectants reaches and interacts with the lipids.

Figure 2 shows the ^{13}C and ^{1}H MAS spectra of control DMPC membranes from 303 to 203 K. The ^{13}C spectra were measured with CP at all temperatures except at 303 K, which was measured with DP. The gel-to liquid-crystalline phase transition temperature (T_m) of DMPC is 296 K, thus significant line broadening was observed below 273 K. The ^{1}H MAS spectra indicate that most DMPC peaks are broadened beyond detection below 253 K, and by 203 K the liquid–water signal is also suppressed, giving a featureless spectrum over the entire chemical shift range.

Trehalose did not enhance the ^{13}C and ^{1}H spectral resolution (Fig. 3a, b). In fact, the 253 K ^{13}C spectra show slightly worse resolution than the unprotected sample. Moreover, the headgroup Cγ signal, which is present in the control spectrum at 203 K, is absent in the trehalose-bound spectrum, suggesting that the trimethylamine may undergo intermediate-timescale motion at 203 K in the trehalose-bound membrane. Water is fully frozen at 203 K.

We attribute the absence of trehalose-induced line narrowing to its non-permeable nature: because it cannot traverse the outermost bilayer, it may not be able to affect the majority of lipids in the multilamellar vesicles. We tested the alternative method of adding trehalose to the vesicle solution before freeze–thaw cycles. However, this procedure was ineffective because trehalose is highly water-soluble and partitions mostly to solution rather than the membrane. When threefold excess trehalose (∼30 mg) was added to the vesicle solution, only ∼2 % of the trehalose bound to the pellet in the end, and no impact on linewidths was observed (data not shown). This observation suggests that varying the concentration of trehalose is unlikely to improve the resolution.

Glycerol, a permeable cryoprotectant, performed moderately better than trehalose, giving rise to higher-resolution spectrum than the control sample at 273 K (Fig. 3c, d). Three resolved carbonyl peaks and doublets for G2 and Cβ are observed, indicating that glycerol creates two discrete conformations in the DMPC headgroup, backbone and the beginning of the acyl chains. These two conformations are likely related to the two isomers in the crystal structures of DMPC (Nomura et al. 2011) and other phosphatidylcholine lipids (Tang et al. 2007). Each isomer can have two different carbonyl chemical shifts due to the inequivalence of *sn*-1 and *sn*-2 chains, thus a maximum of four C′ peaks is possible. Indeed, the three $^{13}C'$ chemical shifts measured here (174.6, 172.9, and 171.6 ppm) agree well with the values reported for crystalline DMPC (175.4, 173.8, 171.8, and 170.6 ppm) and POPC (175.5, 174.6, 173.6, and 171.8 ppm). We consider this bimodal conformational distribution favorable than the single broad distribution of the conformation of the unprotected lipids. The water ^{1}H signal of the glycerol-bound DMPC is sharp down to 253 K, and even at 203 K a small amount of liquid–water signal remains. However, most ^{13}C signals are severely broadened below 273 K, similar to the control membrane. Thus, while glycerol retards ice formation to some extent and reduces the lipid conformation to a bimodal distribution at 273 K, it is not able to maintain this narrow distribution at 203 K, at least at the concentrations used in our sample.

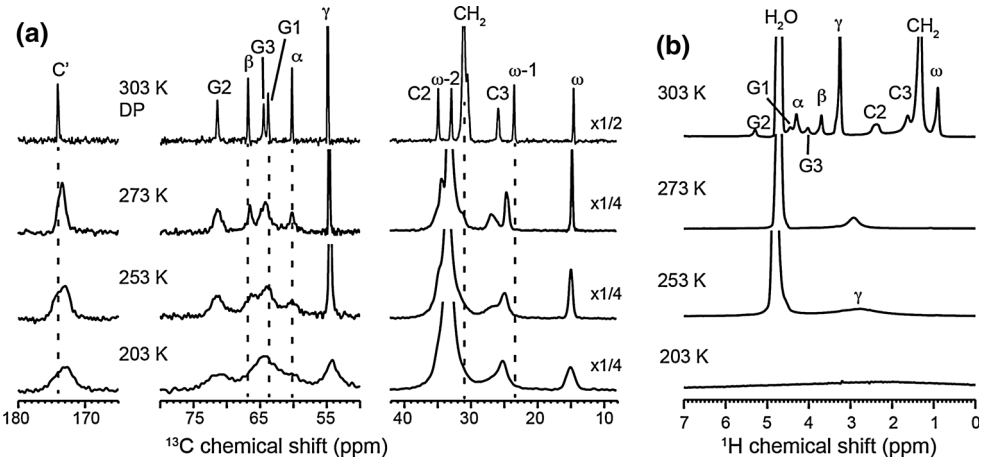

Fig. 2 Variable-temperature ^{13}C (**a**) and ^{1}H (**b**) MAS spectra of control DMPC membranes without cryoprotectants. The ^{13}C spectra were measured with CP at all temperatures except at 303 K, which was measured with DP. Lipid assignments are indicated. Significant line broadening was observed below 273 K. The ^{13}C acyl-chain intensities are plotted using the indicated scaling factors with respect to the rest of the spectra to better represent the peak linewidths

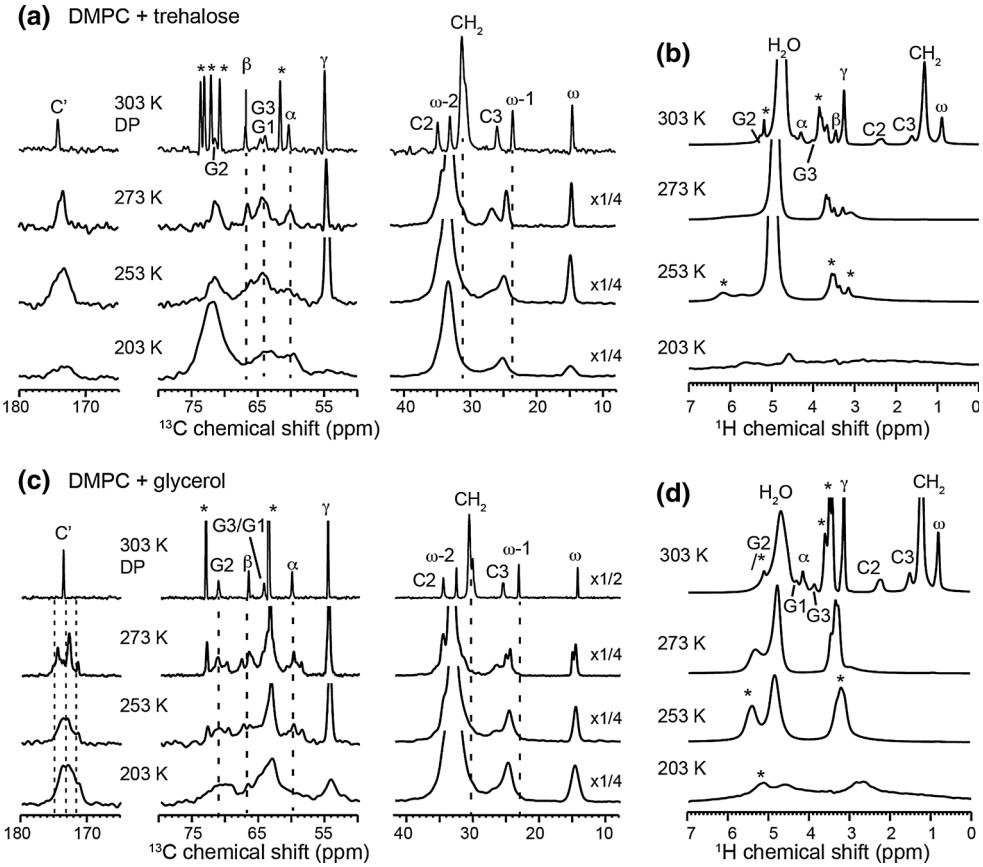

Fig. 3 Variable-temperature ^{13}C (**a**, **c**) and ^{1}H (**b**, **d**) MAS spectra of DMPC membranes containing trehalose (**a**, **b**) and glycerol (**c**, **d**). *Asterisks* indicate cryoprotectant peaks. The trehalose-bound sample showed no linewidth change compared to the control sample in Fig. 2, while the glycerol-bound membrane showed resolution enhancement at 273 K but similar line broadening as the control membrane below 253 K

We next investigated DMSO and DMF-bound DMPC membranes. DMSO is a well studied cryoprotectant (Yu and Quinn 1998), and DMF also exhibits favorable chemical properties for cryoprotection: it is a polar aprotic solvent with a high boiling point, is completely miscible with water, and strongly depresses the freezing point of water. In contrast to trehalose and glycerol, the ^{13}C spectra of DMSO-bound DMPC membranes (Fig. 4a) show relatively narrow headgroup, backbone and C' signals all the way to 203 K, with double peaks for these carbons. At 203 K, the aliphatic ω and ω − 1 signals are also much narrower compared to the control, trehalose- and glycerol-bound membranes, indicating that DMSO not only orders the polar region of the lipid molecule but also partially

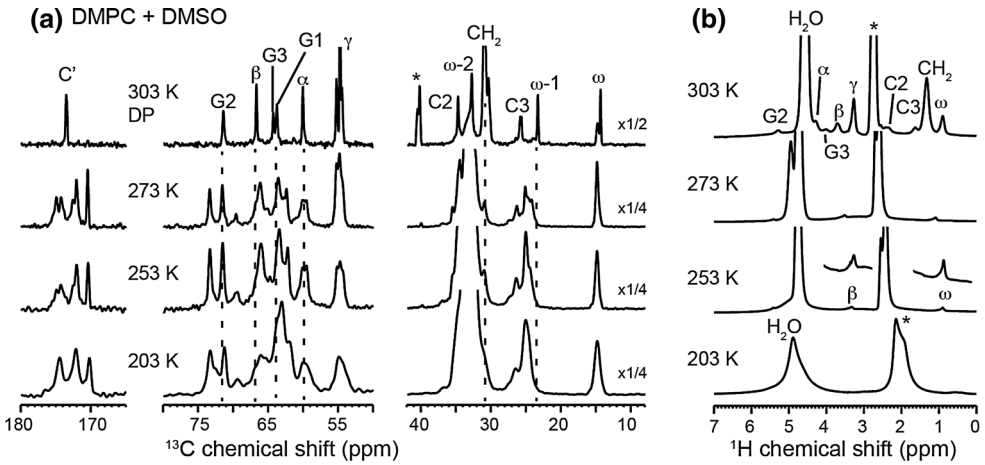

Fig. 4 Variable-temperature ^{13}C (**a**, **c**) and ^{1}H (**b**, **d**) MAS spectra of DMPC membranes containing DMSO (**a**, **b**) and DMF (**c**, **d**). *Asterisks* indicate the cryoprotectant peaks. The DMSO-bound membrane retains significant liquid water at 203 K and has much narrower headgroup and backbone ^{13}C signals at 203 K than the control membrane. DMF shows slightly weaker beneficial effect than DMSO but the lipid spectra are still better resolved than the control spectra

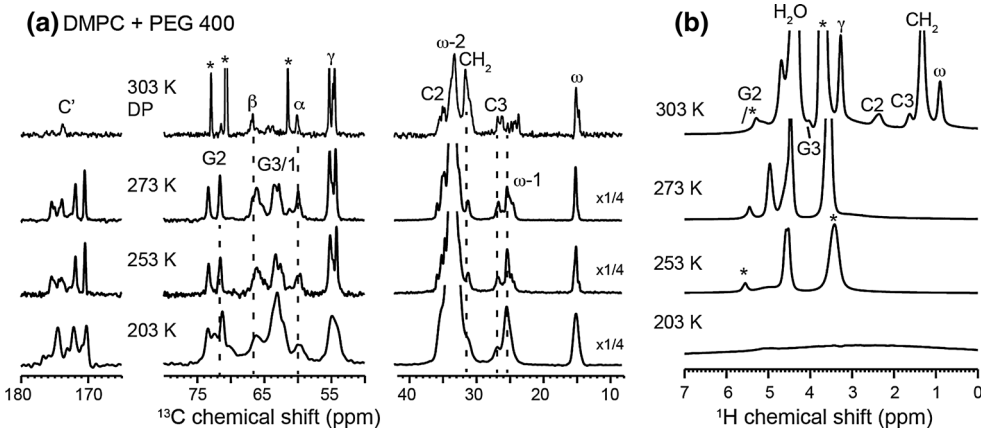

Fig. 5 Variable-temperature ^{13}C (**a**) and ^{1}H (**b**) MAS spectra of PEG-protected DMPC membrane. *Asterisks* indicate PEG peaks. The DP spectrum at 303 K shows low headgroup intensities, indicating that PEG immobilizes the headgroup above the phase-transition temperature. At 203 K, PEG retains good lipid spectral resolution but does not prevent ice formation

orders the hydrophobic chains. ^{1}H spectra (Fig. 4b) show well-resolved headgroup β and acyl-chain ω signals at 253 K, indicating that the lipids are partly mobile at this temperature. At 203 K, significant liquid–water ^{1}H signal remains, indicating that DMSO efficiently suppresses ice formation. The DMF-bound DMPC sample performed similarly well as DMSO, although the ^{13}C spectral resolution is slightly worse at 203 K (Fig. 4c, d).

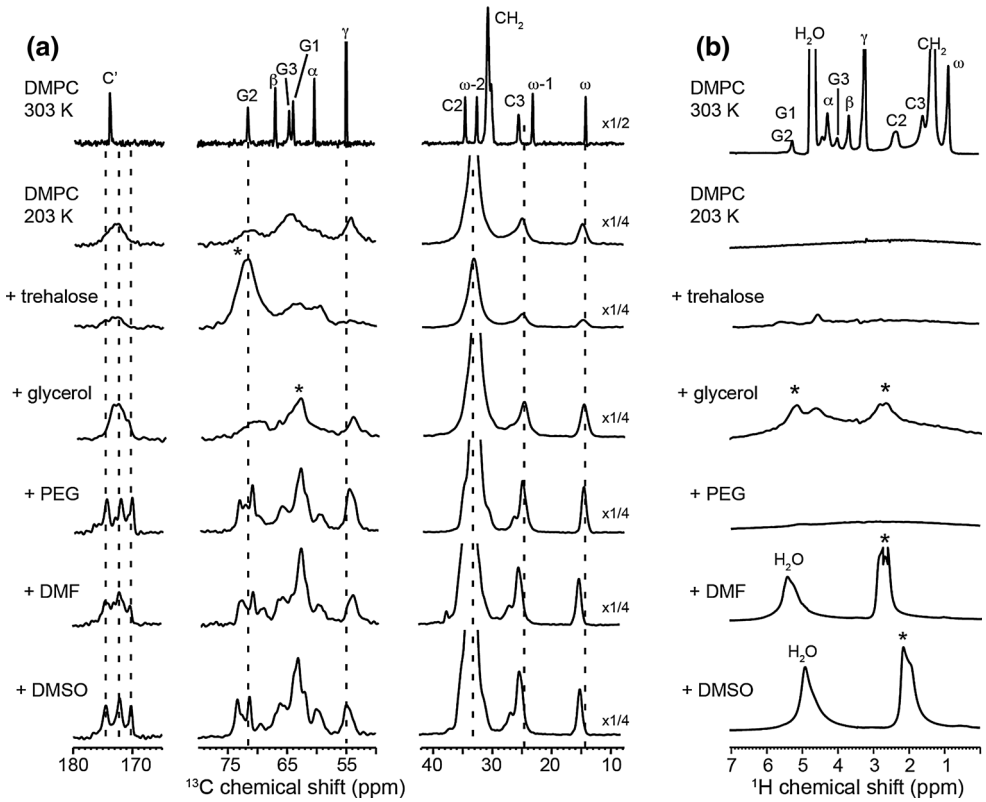

Fig. 6 Comparison of DMPC ^{13}C (**a**) and ^{1}H (**b**) MAS spectra in the absence (*top two rows*) and presence of cryoprotectants. The 303 K spectrum of the control sample gives the limiting resolution of the liquid-crystalline membrane. All other spectra were measured at 203 K. The unprotected sample shows severe line broadening at 203 K, and water is completely frozen. Trehalose and glycerol did not cause any resolution enhancement, while PEG, DMF and DMSO improved the spectral resolution. DMF and DMSO also retained liquid water, indicating that they retard ice formation

Figure 5 shows the spectra of PEG-400-bound DMPC membrane. Interestingly, at 303 K, the ^{13}C DP spectra have weak intensities, indicating that the lipids are significantly immobilized by PEG-400. Between 273 and 253 K, four resolved carbonyl peaks and G2, Cγ and Cα doublets are detected, similar to the DMSO- and DMF-protected membranes. At 203 K, the lipid ^{13}C signals remained sharp, but no liquid–water ^{1}H signal remains. Thus, PEG is less efficient than DMSO and DMF in preventing ice formation, but this does not prevent it from inducing ordered lipid conformations. We speculate that this anomalous behavior may result from the larger molecular weight of PEG-400, which should allow it to span the membrane more than the other cryoprotectants, so that the lipids may be ordered even in the presence of ice crystals.

Figure 6 compares the 203 K ^{13}C and ^{1}H spectra of the DMPC membranes in the absence and presence of the five cryoprotectants. Except for trehalose, the other four cryoprotectants showed varying degrees of resolution enhancement. Based on the ^{13}C linewidths, the cryoprotecting potency increases in the order of glycerol < DMF < PEG ~ DMSO. To compare the linewidths of the different cryoprotected samples quantitatively, we plotted the 203 K ^{13}C linewidths (full width at half maximum) of Cγ, CH_2 and ω (Fig. 7a), which report the structural order of the lipid headgroup, acyl chain, and the chain end, respectively. For all samples, Cγ and CH_2 exhibit the largest linewidths, while ω has the narrowest linewidths. Focusing on the DMSO-protected membrane, the temperature-dependent linewidths of various sites are compared in Fig. 7b. The headgroup Cγ shows the largest linewidths in the gel phase whereas the backbone G2 has the smallest linewidths. Given the proximity of G2 and Cγ, this result indicates that DMSO exerts divergent effects within a small volume, ordering the lipid backbone while disordering the headgroup. G2 and ω linewidths increase relatively slowly with decreasing temperature, while CH_2 and Cγ linewidths increase sharply below ~273 K. The water ^{1}H linewidth surged only below 223 K, consistent with the freezing point of the DMSO-water solution. The fact that the water linewidth change does not correlate with the lipid linewidth changes confirms that the low-temperature lipid structural disorder is partly independent of ice formation. To quantify the degree of line narrowing by DMSO, we compared the temperature-dependent linewidths between the unprotected and DMSO-protected DMPC samples (Fig. 7c). The largest linewidth reduction is found at C' and G2. In comparison, the hydrophobic chains show modest line narrowing in this temperature range. On the other hand, the small slopes of the ω and CH_2 curves of the DMSO-protected sample suggest that below 200 K, the cryoprotectant may manifest a larger line-narrowing effect.

To test the hypothesis that cryoprotectants enhance low-temperature spectral resolution by reducing conformational dynamics at high temperature, we measured site-specific C–H order parameters of DMPC using the DIPSHIFT experiment. The experiments were conducted at 280 K,

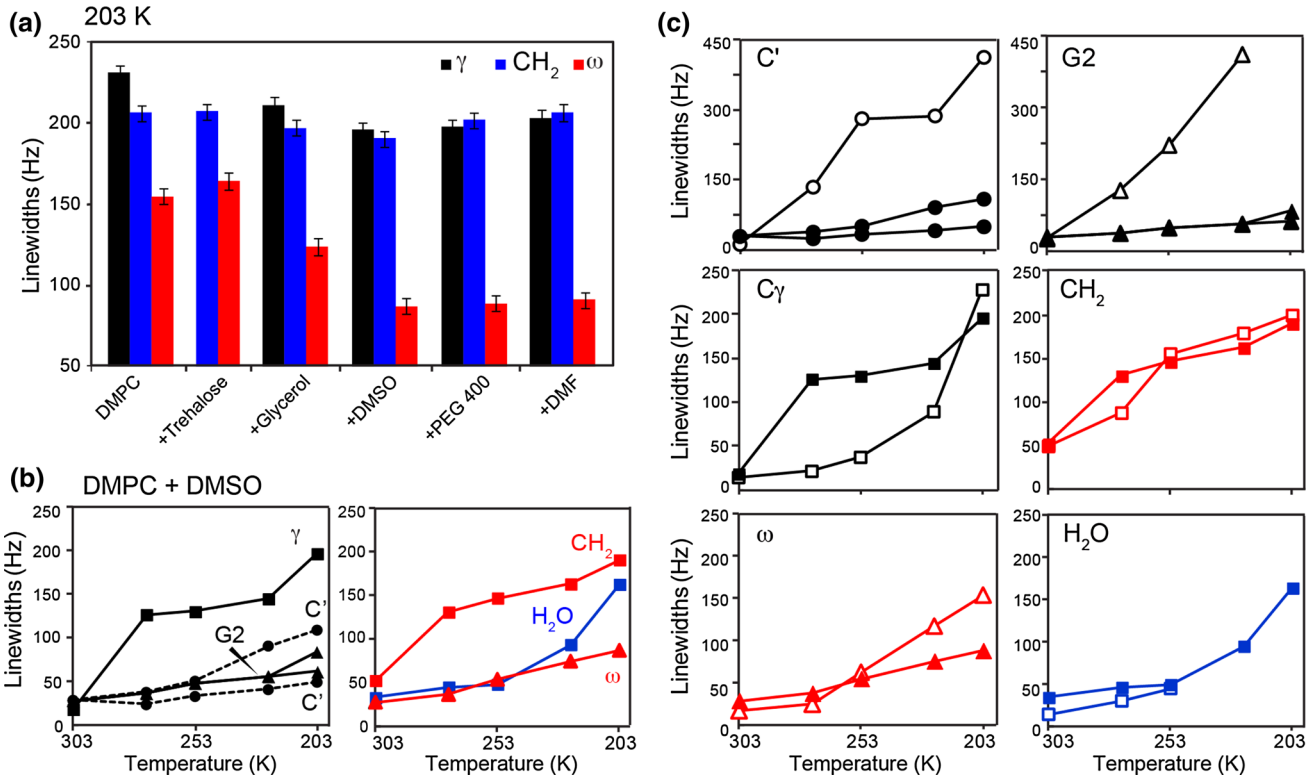

Fig. 7 Comparison of ^{13}C and ^{1}H linewidths of DMPC bound to different cryoprotectants and at different temperatures. **a** Cryoprotectant comparison at 203 K. The Cγ, CH_2 and ω linewidths are plotted. DMSO and PEG-400 induce the narrowest lipid linewidths. **b** Temperature dependence of the ^{13}C linewidths of DMSO-bound DMPC and the ^{1}H linewidths of water. Two linewidths are plotted for G2 and C′ due to the presence of two conformations. **c** Comparison of DMSO-bound (*filled symbols*) and control (*open symbols*) DMPC ^{13}C linewidths and water ^{1}H linewidths as a function of temperature. The C′ and glycerol backbone G2 show the largest linewidth reduction by cryoprotection

below the T_m of DMPC, to obtain sufficient CP intensities and to avoid making the order parameters too small to be accurate. Figure 8 shows the ^{13}C–^{1}H dipolar dephasing curves of several sites, ω − 1, CH_2, G2, and Cβ, which represent the acyl chains, glycerol backbone, and headgroup of the lipid. As expected, the chain-end ω − 1 in the control sample exhibits shallow dephasing curves, indicating small C–H order parameters (S_{CH}) due to large-amplitude motion. G2 has the deepest dephasing, corresponding to the strongest C–H dipolar coupling or the largest S_{CH}, consistent with the relative rigidity of the lipid backbone. When glycerol is added to the membrane, most sites show similar couplings as the control sample, indicating that glycerol has little impact on lipid dynamics. This is correlated with the weak line-narrowing effect. In comparison, PEG-400 and DMSO significantly increased the dipolar couplings of all segments. The change at the headgroup Cβ is especially large, with S_{CH} increasing from 0.51 for the control sample to 0.65 for the PEG-bound sample and 0.93 for the DMSO-bound membrane. Similarly, the G2 order parameters increased to ∼0.93 for PEG- and DMSO-protected membranes. These results indicate unambiguously that DMSO and PEG-400 intercalation into the membrane-water interface immobilizes the lipid backbone and headgroup. PEG-400 differs slightly from DMSO in the exact headgroup moiety affected (Fig. 8f): DMSO immobilizes Cβ more whereas PEG immobilizes Cα more. ^{31}P spinning sideband spectra at 273 K (Fig. 8e), support the DIPSHIFT data, showing that all three cryoprotected samples have higher sideband intensities than the control membrane, but DMSO- and PEG-bound samples have larger CSAs than the glycerol-bound sample. Therefore, the better line-narrowing compounds immobilize the lipids more strongly.

In addition to larger order parameters, PEG-400 and DMSO also affected the T_2 decays of the DIPSHIFT dephasing curves, as manifested by an intensity drop at the end of the rotor period for most sites. This intensity asymmetry is known to be caused by motion on the timescale of the inverse of the dipolar coupling (deAzevedo et al. 2008). The faster T_2 decay of the DMSO- and PEG-bound samples is particularly clear for acyl chain sites. Therefore, although the acyl chains have not reached their rigid limit at 280 K, the remaining motions are slowing down to the intermediate regime, again indicating cryoprotectant-induced reduction in the dynamic disorder.

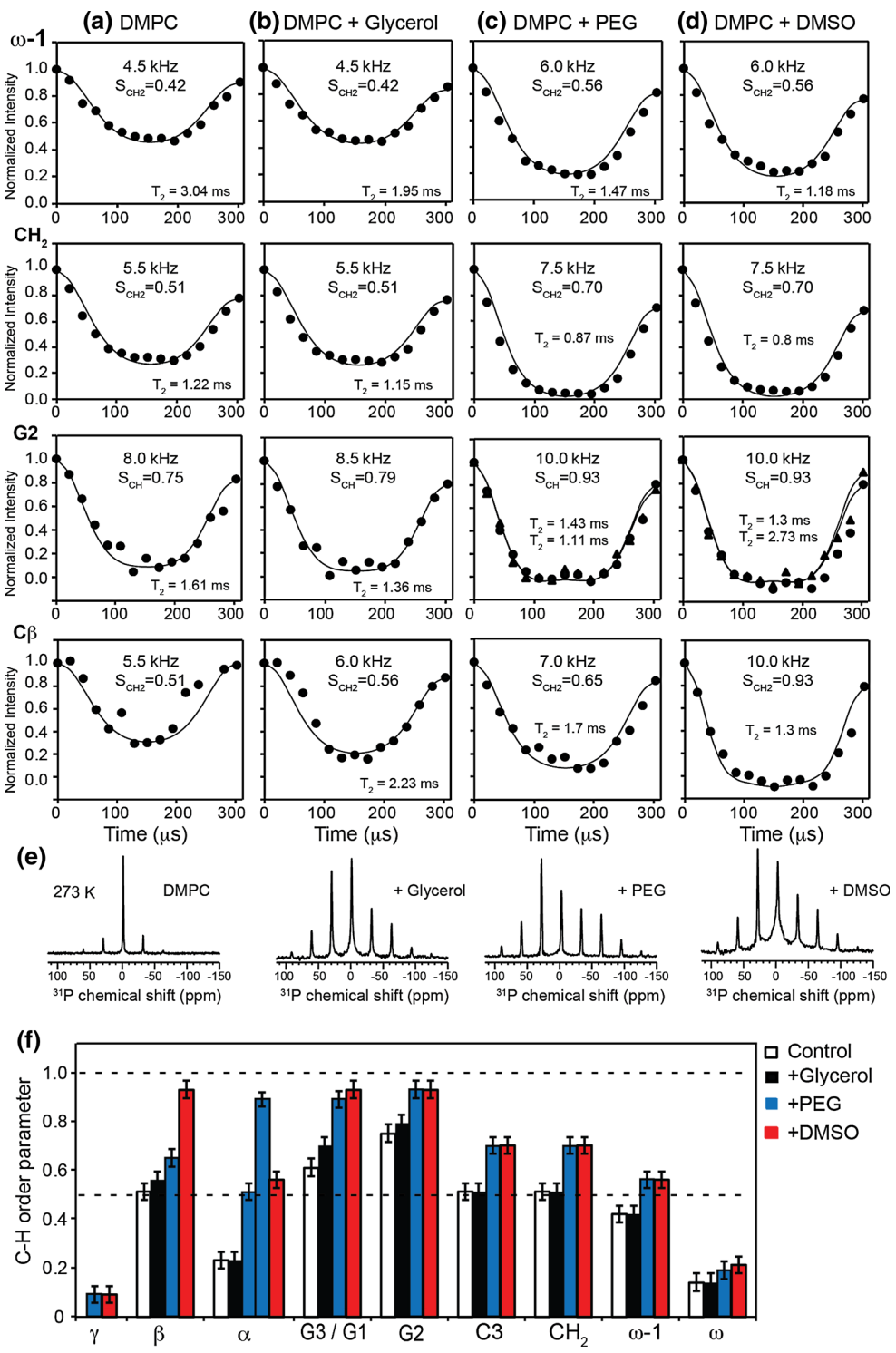

Fig. 8 Cryoprotectants partially immobilize lipids. **a**–**d** ^{13}C–^{1}H dipolar couplings of DMPC membranes in the absence and presence of cryoprotectants. The data were obtained at 280 K under 3.3 kHz MAS. From *left* to *right*, the columns correspond to **a** control DMPC membrane, **b** glycerol-bound membrane, **c** PEG-400 bound membrane, and **d** DMSO-bound membrane. *Solid lines* are best-fit simulations with empirical T_2 decay constants indicated. Glycerol-bound DMPC exhibits similar order parameters as the control membrane while PEG-400 and DMSO give rise to larger dipolar couplings, indicating immobilization of the lipid. **e** ^{31}P MAS spectra of the four membranes at 273 K, showing larger sideband intensities for the cryoprotected samples than the control sample. **f** C–H order parameters of the four samples at 280 K for all resolved signals. *Dashed lines* guide the eye for the rigid limit ($S_{CH} = 1.0$) and $S_{CH} = 0.50$. For the control DMPC sample and the glycerol-bound DMPC sample, most sites exhibit S_{CH} values lower than 0.5, while the PEG- and DMSO-bound DMPC samples have S_{CH} values between 0.5 and 1.0 except for the chain end ω and the headgroup Cγ

Interaction of DMSO with other phosphatidylcholine lipids

We investigated DMSO interaction with two other phosphatidylcholine lipids, DOPC and DLPC, to assess whether chain unsaturation and chain length affect cryoprotection. DLPC has 12 carbons per chain and a T_m of 272 K, while the 18-carbon DOPC contains one double bond per chain and has a low T_m of 253 K. The control DOPC ^{13}C spectra show narrower lines than DMPC at 203 K (Fig. S1), as expected because of the ~40 K lower transition temperature than DMPC. DMSO binding did not change the

spectral resolution significantly, but the peaks are slightly better resolved than the DMSO-bound DMPC spectrum at the same temperature. Only a single conformer is detected in the headgroup and backbone. Given the modest effect of DMSO on the DOPC spectra, and resolution difference between DOPC and DMPC is purely due to the 40 K T_m difference, we hypothesize that the DOPC linewidths at 160 K will approach the DMPC linewidths at 200 K. DMSO also caused modest changes to the DLPC linewidths, but peak doubling is seen in the carbonyl and glycerol backbone region, similar to the DMSO-protected DMPC sample. We attribute the reduced line-narrowing ability of DMSO to DLPC and DOPC membranes to a combination of the larger chain disorder of the two lipids and the moderately larger amount of DMSO used (Table 1), since high cryoprotectant concentrations can cause lateral expansion of the lipid membrane and increase the lipid conformational disorder.

Interaction of DMSO with negatively charged membranes

We applied DMSO, DMF and PEG-400 to DOPC/DOPG membranes to investigate the interaction of negatively charged lipids with cryoprotectants. The DMSO and PEG samples contained moderately higher cryoprotectant concentrations than the protected DMPC samples (Table 1). The ^{13}C spectra of the DOPC/DOPG membrane with and without cryoprotectants are shown in Fig. S2. None of the three cryoprotectants caused significant line narrowing compared to the control membrane. We attribute this result to electrostatic repulsion between the anionic lipids and the polar moieties of the cryoprotectants, which weakens cryoprotectant binding. This is consistent with resonance energy transfer data that DMSO does not protect vesicles containing 30 % negatively charged phosphatidylserine (Anchordoguy et al. 1987, 1991). The ^{1}H spectra show residual water intensities at 203 K for the DMSO- and DMF-bound samples, similar to the DMSO- and DMF-protected DMPC samples. However, the water peaks are lower in the protected DOPC/DOPG membranes. This can be explained by the different cryoprotectant concentrations used between the two membranes. The DMSO-protected DOPC/DOPG sample contains less water than the corresponding DMPC sample, while the DMF concentration used in the DOPC/DOPG sample should increase the water freezing point compared to the corresponding DMPC sample.

Interaction of DMSO with the DLPE membrane

The above data suggest that neutral lipids, saturated chains and high T_m are favorable properties for reducing the lipid conformational disorder under cryoprotection. These factors led us to examine DLPE spectral quality under cryoprotection. The amine moiety in the PE headgroup allows the formation of intermolecular hydrogen bonds, which orders the lipid packing and increases the T_m of PE compared to PC lipids with the same acyl chains. DLPE has a T_m of 302 K, which is 30 K higher than the DLPC T_m. PE lipids also differ from PC lipids in having a smaller headgroup, which causes negative spontaneous curvature, which may counter the positive curvature of interfacially bound cryoprotectants. The measured ^{13}C MAS spectra bear out these predictions. The control DLPE sample exhibits crystalline-like spectra at 298 K, with four resolved $^{13}C'$ signals and peak-doubling for G2, Cα and ω (Fig. 9a, b). Thus, gel-phase DLPE adopts two conformations for both the polar and non-polar parts of the molecule. The four $^{13}C'$ chemical shifts seen here (173.3, 172.2, 170.5, and 168.8 ppm) agree with those reported for crystalline L-α-DPPE within 0.4 ppm (Bruzik and Harwood 1997; Nomura et al. 2011). The ^{13}C spectral resolution is largely retained at 203 K, except for the acyl-chain signals, which show moderate broadening. Interestingly, the water ^{1}H peak is completely broadened in the unprotected membrane below 223 K, despite the good ^{13}C resolution. DMSO binding enhanced the ^{13}C spectral resolution (Fig. 9c, d) and maintained it down to 203 K: the four $^{13}C'$ signals are resolved to the baseline and the acyl-chain signals are much sharper than in the unprotected sample. For example, the C2 and ω − 2 peaks are resolved from the CH_2 signal, which is not observed in any other samples' spectra. The ω signal retained the doublet splitting throughout the temperature range. Finally, the DMSO-protected membrane shows a strikingly narrow water peak from 293 to 203 K, unaffected by temperature. Thus, the DMSO-protected DLPE membrane is highly ordered and ice formation is fully prevented at ∼200 K, making this system a promising medium for low-temperature membrane proteins NMR studies.

Effects of DMSO on membrane-bound M2TM

To investigate the effects of one of the best cryoprotectants, DMSO, on membrane peptides, we measured the ^{13}C and ^{15}N spectra of M2TM and PG-1 bound to DMPC and DLPE membranes. The D44A-M2TM sample contains ^{13}C, ^{15}N-labeled L26, V27, S31, G34, and A44. Among these residues, L26, V27 and A44 lie at the membrane-water interface whereas G34 resides in the middle of the lipid bilayer. Based on the heptad repeat of this four-helix bundle, V27 and G34 face the pore of the helical bundle while the other three residues lie at the helix–helix interface (Cady and Hong 2008, 2009; Luo and Hong 2010). Figure 10a, b shows the ^{13}C spectra of M2TM-containing

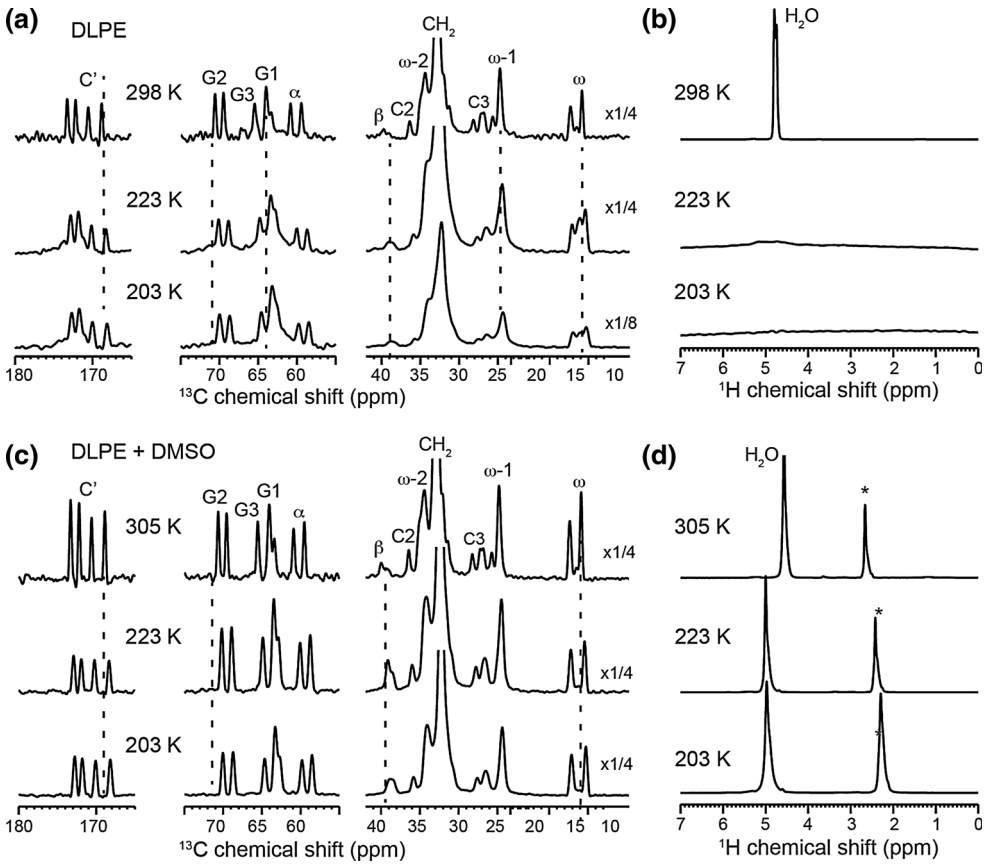

Fig. 9 Variable-temperature ^{13}C (**a**, **c**) and ^{1}H (**b**, **d**) MAS spectra of DLPE membranes without (**a**, **b**) and with DMSO (**c**, **d**). The DMSO-bound sample maintained high-resolution ^{13}C spectra at 203 K, and the liquid–water peak is preserved and sharp. The unprotected sample lost the water peak altogether at 203 K, but the ^{13}C resolution is still good compared to the DMSO-bound DMPC membrane

membranes. At 210 K, DMSO caused residue-specific line narrowing in both DMPC and DLPE membranes: the G34 Cα, A44 Cβ, and V27 Cα linewidths decreased by 0.5–1.5 ppm, while other sites show less visible linewidth change. Consistent with the ^{13}C spectra, the ^{15}N spectra show significant line narrowing (Fig. 10c, d), especially at 283 K for the DLPE samples, where the main 119-ppm ^{15}N peak sharpened from 6.3 to 4.2 ppm due to DMSO cryoprotection.

At the moderate temperature of 273 K, the ^{13}C CP spectra of the DMPC samples show the same line narrowing and peak doubling for G2, C′ and Cβ as found in peptide-free samples. Thus, DMSO affects the membrane in the same way between the peptide-bound and peptide-free samples, and conclusions about cryoprotectant effects from the lipid-only spectra can be extended to peptide-containing membranes.

Interestingly, comparison of the 273 and 210 K ^{13}C spectra indicate that the M2 ^{13}C linewidths are relatively unchanged by temperature in the cryoprotected samples: the linewidths increased by only ∼0.3 ppm over the 63 K temperature decrease. In contrast, the unprotected DMPC sample increased the linewidths by ∼1.3 ppm for V27 Cα and A44 Cβ over this temperature range. Thus, DMSO, and by implication the other two effective cryoprotectants, PEG and DMF, does not narrow lines at high temperature but maintains the same linewidths at low temperature.

The line narrowing of G34 seen at both moderate and low temperatures by cryoprotection is noteworthy from a structural point of view. It is known that G34 in the M2TM four-helix bundle exhibits at least two conformations, depending on environmental factors such as membrane thickness, pH, and the absence or presence of drugs (Hu et al. 2007, 2011). A kinked helical structure called state 1 is promoted by thick bilayers, high pH, and drug binding; a straight helix with large tilt angles but non-ideal conformation at H37 (state 2) is promoted by high pH, thin bilayers, and the absence of drug; while a straight helix with ideal helical conformation at H37 (state 3) is found at low pH. States 2 and 3 have the same G34 chemical shifts, which match the DMSO-bound G34 $^{13}C\alpha$ and ^{15}N chemical shifts measured here. Thus, in both DMPC and DLPE membranes, DMSO selects the straight-helix conformation at residue 34, which is consistent with the relatively short chains of these lipids, the high pH, and the lack of drug in these samples. The fact that the G34 signals are broad in the unprotected membranes even at moderate temperatures (283–243 K) indicates that all three states are significantly populated in the absence of cryoprotection. In our experience, such conformational heterogeneity is common for

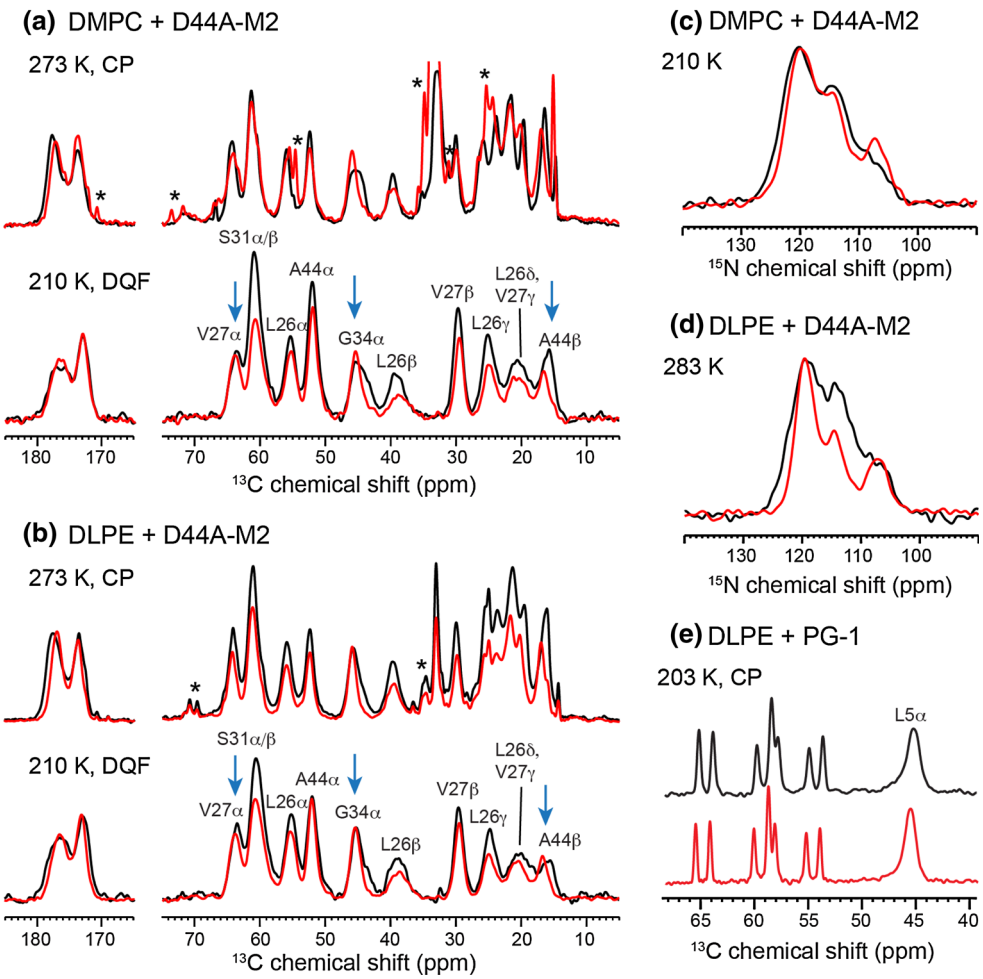

Fig. 10 ^{13}C and ^{15}N MAS spectra of DMPC and DLPE membranes containing D44A-M2TM or PG-1. The spectra of cryoprotectant-free samples (*black*) are overlaid with the spectra of DMSO-bound membranes (*red*). **a** 273 K ^{13}C CP spectra and 210 K ^{13}C DQF spectra of M2TM-containing DMPC membranes. *Asterisks* indicate lipid peaks in the ^{13}C CP spectra. **b** 273 K ^{13}C CP spectra and 210 K ^{13}C DQF spectra of M2TM-containing DLPE membranes. G34, A44 and V27 peaks (*blue arrows*) show significant line narrowing by DMSO, while other residues have limited resolution change. **c** ^{15}N CP spectra of DMPC-M2TM samples at 210 K. **d** ^{15}N CP spectra of the DLPE-M2TM samples at 283 K. **e** 203 K ^{13}C CP spectra of PG-1 containing DLPE membranes without (*black*) and with (*red*) DMSO. The L5 Cα signal does not shown significant line narrowing by DMSO

many membrane peptides. It is not clear to what extent such heterogeneity is intrinsic to the protein sequences and the lipid membranes used. Cryoprotection may be a way to gain insight into this question.

The L5 Cα signal of PG-1 (Fig. 10e) in the DLPE membrane at 210 K showed no significant linewidth reduction by DMSO. For the protected sample, the Cα linewidth is 1.3 ppm, compared to 0.8 ppm at 283 K (data not shown). Since L5 is located in the well-defined and rigid β-strand core of this peptide (Hong and Su 2011; Tang and Hong 2009), and the Cα label has no line broadening from ^{13}C–^{13}C J-coupling, the 0.5-ppm linewidth increase over this ~73 K temperature drop gives an indication of the contribution of static conformational disorder to linewidths for a rigid membrane peptide.

Discussion

The above spectra provide the first database of the utilities of several common cryoprotectants for SSNMR studies of membrane peptides and proteins. Among the five cryoprotectants examined, trehalose is a commonly used disaccharide in cell cryopreservation, and glycerol/water matrix is a common antifreeze solution. But under our sample preparation conditions, trehalose had no detectable effect on lipid linewidths, whereas glycerol enhanced the resolution only at moderate temperatures (~273 K) but did not prevent line broadening at ~200 K. Trehalose' limited effect is most likely due to the non-permeable nature of the sugar, which makes it contact only a small fraction of all lipids. At 273 K where glycerol caused line narrowing, the ^{13}C spectra resemble the 203 K-spectra of DMSO- and PEG-bound DMPC membranes. This suggests that glycerol's cryoprotecting ability is shifted by ~70 K higher than that of DMSO and PEG. We hypothesize that this temperature shift is due the higher freezing point of the glycerol/water mixture (Table 1): glycerol depresses the water freezing point maximally to 226 K while DMSO and PEG depress the freezing points maximally to 218 K and 203 K, respectively. At the glycerol/water ratio used in our sample, the freezing point is about 245 K. If the optimal glycerol concentration of ~67 wt% is used, the freezing point should be depressed by another 20 K, which should

give high-resolution ^{13}C spectra down to ~253 K. If verified, this would imply that ice formation and the resulting disordering of biomolecular structure remains a significant source of line broadening at low temperature.

The other three permeable cryoprotectants showed considerable line-narrowing effects on lipids, with DMSO and PEG-400 inducing the narrowest ^{13}C linewidths while DMSO and DMF giving the narrowest water ^{1}H peaks. All three cryoprotectants gave rise to two peaks each for various headgroup, backbone and carbonyl carbons, indicating that these molecules intercalate between lipids at the membrane-water interface in such a way to promote two isomers. The two conformations are likely similar to those seen in the crystalline state for POPC and DMPC based on the similar chemical shifts (Tang et al. 2007; Bruzik and Harwood 1997; Nomura et al. 2011). The interfacial location of cryoprotectants is consistent with X-ray diffraction data (Yu and Quinn 2000) and molecular dynamics simulations of DMSO-bound membranes (Kyrychenko and Dyubko 2008). At this interfacial location, the polar groups of cryoprotectants can form hydrogen bonds with the lipid headgroup and backbone, thus locking lipids into a small number of conformations. Indeed, lipid rigidification is verified by C–H dipolar couplings and ^{31}P CSAs, which show that the better line-narrowing compounds—DMSO and PEG—also cause larger order parameters than in the unprotected and glycerol-protected membranes. Infrared spectra showed that DMSO reduces the CH_2 vibrational frequency of PC chains, also indicating decreased membrane fluidity (Anchordoguy et al. 1992). These results support the notion that reducing lipid conformational dynamics at high temperature enhances the spectral resolution at low temperature. The interfacial location of DMSO, DMF and PEG-400 may also partly account for the excellent linewidths of DLPE, whose smaller headgroup compared to phosphatidylcholine lipids favors cryoprotectant binding. Among the high-performing cryoprotectants, PEG is often used in membrane protein X-ray crystallography (Long et al. 2007; Rasmussen et al. 2011; Wang et al. 2013a, b), which also verify its ability to create ordered protein structures in membrane-mimetic environments.

Low-temperature ^{1}H spectra indicate that DMSO and DMF are more efficient than glycerol and PEG in preventing ice formation (Fig. 6). This is consistent with the trend of freezing-point depression by these compounds. Molecular dynamics simulations indicate that cryoprotectants with similarly high water miscibility can have different molecular interactions with water: DMSO equilibrates with water much faster than glycerol and ethylene glycol (Kyrychenko and Dyubko 2008).

DMSO is one of the best-studied membrane additives, not only as a cryoprotectant but also as a fusogen and permeability-enhancing agent (Gordeliy et al. 1998; Yu and Quinn 1998), and these functions are active at different concentrations and temperatures. Interestingly, DMSO thins lipid membranes (Gordeliy et al. 1998) but increases their T_m (Chang and Dea 2001). This apparent contradiction is proposed to be resolved by the fact that the DMSO/water solution increases inter-membrane interactions. The intricacy of DMSO interactions with lipids and water at the membrane-water interface may account for its ability to simultaneously produce well-ordered lipid conformations and prevent ice formation at low temperature. In comparison, PEG-400 yielded high resolution for the lipid spectra, but did not prevent ice formation, while DMF prevented ice formation but did not give as high-resolution lipid spectra as DMSO.

Compared to its action on lipids, DMSO caused more site-specific line narrowing of the influenza M2 peptide. Residues G34, A44, and V27 showed significant linewidth reduction over unprotected membranes, while S31 and L26 had limited changes. V27 and A44 lie at the membrane-water interface where the cryoprotectant binds, thus their linewidth reduction is likely due to direct structural ordering of this part of the membrane. However, G34 is in the middle of the transmembrane helix and thus the hydrophobic center of the bilayer, where the dynamic disorder is the largest (Cady and Hong 2009). Even with DMSO bound the chain-end ω S_{CH} is only 0.21, which is not much larger than the S_{CH} of 0.14 for the unprotected membrane (Fig. 8f). Thus, the significant line narrowing of G34 reflects conformational ordering of the entire helix as transmitted from the immobilization of the lipid headgroup and backbone, instead of direct interactions between DMSO and the peptide.

The observation that cryoprotected M2 has similar linewidths at 273 and 210 K while the unprotected sample broadened significantly over this temperature range (Fig. 10) is illuminating and confirms the beneficial effect of cryoprotection. It is also noteworthy that the residues with the most significant line narrowing also had the broadest linewidths in the unprotected state. Thus, cryoprotection appears to equalize the linewidths, by creating a more uniformly ordered protein structure.

In general, membrane peptides such as M2TM are more disordered than larger proteins, because their small size leads to more extensive interactions with lipids. In addition, the M2 protein sequence inherently encodes significant conformational plasticity (Stouffer et al. 2005) due to its proton-channel function (Hong and Degrado 2012). We believe these factors account for the >1-ppm linewidths of most residues in M2TM, with or without cryoprotectants. The fact that visible line narrowing is achieved for the most disordered residues, despite the inherent conformational plasticity of the molecule, suggests that DMSO should have significant cryoprotecting abilities to other membrane peptides and proteins as well. Experiments well below

$\sim$200 K will be interesting, to determine whether at cryogenic temperature the linewidths will improve over the unprotected samples.

Conclusions

We investigated the effects of five cryoprotectants on the NMR linewidths of lipid membranes and membrane peptides from ambient temperature to 203 K. For DMPC membranes, DMSO induced the narrowest ^{13}C linewidths, followed by PEG and DMF, while glycerol and trehalose did not prevent low-temperature-induced line broadening. DMSO ordered the glycerol backbone and the beginning of the acyl chains most strongly, consistent with the interfacial location of this cryoprotectant. High spectral resolution at $\sim$200 K is best achieved by neutral lipids with intermolecular hydrogen bonds and saturated chains. DMSO prevented line broadening of M2TM from 273 to 210 K, and specifically narrowed the linewidths of residues with large conformational disorder in the unprotected membrane. The PG-1 spectra indicate that a $\sim$70 K temperature drop increases the linewidth by $\sim$0.5-ppm for a rigid membrane peptide. These data indicate that suitable cryoprotectants can enhance spectral resolution at low temperature, by reducing the dynamic conformational disorder at high temperature. DLPE is found to give very high-resolution spectra both in the absence and presence of cryoprotectants, suggesting that this lipid may be a good medium for membrane protein SSNMR. The three most effective cryoprotectants found here are useful not only at $\sim$200 K but also at moderate low temperatures, as seen by the ^{15}N spectra of M2TM at 283 K. Whether these cryoprotectants significantly narrow membrane protein NMR linewidths at $\sim$100 K will need to be tested. Since membrane-protein structures are influenced not only by water but also by lipid membranes, we expect cryoprotectants to be able to enhance spectral resolution below the minimum freezing point of the cryoprotectant/water solution.

The parameter space for optimizing membrane cryoprotectants is large. The current study used cryoprotectant concentrations that deviate from the composition of the minimum water freezing point. Future work can explore the optimal concentrations of cryoprotectants relative to water and lipids, the freezing method, and the development of compounds that not only order the membrane-water interface but also the membrane hydrophobic interior, in order to obtain high-resolution spectra below 100 K.

Acknowledgments The authors thank Dr. Paul White and Dr. Hongwei Yao for suggestions and experimental assistance. This work is funded by NIH grants GM066976 and GM088204 to M. H.

References

Anchordoguy T, Rudolph AS, Carpenter JF, Crowe JH (1987) Modes of interaction of cryoprotectants with membrane phospholipids during freezing. Cryobiology 24:559–560

Anchordoguy TJ, Cecchini CA, Crowe JH, Crowe LM (1991) Insights into the cryoprotective mechanism of dimethyl-sulfoxide for phospholipid-bilayers. Cryobiology 28:467–473

Anchordoguy TJ, Carpenter JF, Crowe JH, Crowe LM (1992) Temperature-dependent perturbation of phospholipid-bilayers by dimethylsulfoxide. Biochim Biophys Acta 1104:117–122

Bajaj VS, van der Wel PC, Griffin RG (2009) Observation of a low-temperature, dynamically driven structural transition in a polypeptide by solid-state NMR spectroscopy. J Am Chem Soc 131:118–128

Baudot A, Boutron P (1998) Glass-forming tendency and stability of aqueous solutions of diethylformamide and dimethylformamide. Cryobiology 37:187–199

Bruzik KS, Harwood JS (1997) Conformational study of phospholipids in crystalline state and hydrated bilayers by C-13 and P-31 CP-MAS NMR. J Am Chem Soc 119:6629–6637

Cady SD, Hong M (2008) Amantadine-induced conformational and dynamical changes of the influenza M2 transmembrane proton channel. Proc Natl Acad Sci USA 105:1483–1488

Cady SD, Hong M (2009) Effects of amantadine binding on the dynamics of bilayer-bound influenza A M2 transmembrane peptide studied by NMR relaxation. J Biomol NMR 45:185–196

Cady SD, Schmidt-Rohr K, Wang J, Soto CS, DeGrado WF et al (2010) Structure of the amantadine binding site of influenza M2 proton channels in lipid bilayers. Nature 463:689–692

Carver TR, Slichter CP (1956) Experimental verification of the overhauser nuclear polarization effect. Phys Rev 102:975–980

Chang HH, Dea PK (2001) Insights into the dynamics of DMSO in phosphatidylcholine bilayers. Biophys Chem 94:33–40

deAzevedo ER, Saalwachter K, Pascui O, de Souza AA, Bonagamba TJ et al (2008) Intermediate motions as studied by solid-state separated local field NMR experiments. J Chem Phys 128:104505

Dick-Perez M, Zhang YA, Hayes J, Salazar A, Zabotina OA et al (2011) Structure and interactions of plant cell-wall polysaccharides by two- and three-dimensional magic-angle-spinning solid-state NMR. Biochemistry 50:989–1000

Franks WT, Zhou DH, Wylie BJ, Money BG, Graesser DT et al (2005) Magic-angle spinning solid-state NMR spectroscopy of the beta1 immunoglobulin binding domain of protein G (GB1): 15 N and 13C chemical shift assignments and conformational analysis. J Am Chem Soc 127:12291–12305

Gordeliy VI, Kiselev MA, Lesieur P, Pole AV, Teixeira J (1998) Lipid membrane structure and interactions in dimethyl sulfoxide/water mixtures. Biophys J 75:2343–2351

Hong M, Degrado WF (2012) Structural basis for proton conduction and inhibition by the influenza M2 protein. Protein Sci 21:1620–1633

Hong M, Griffin RG (1998) Resonance assignment for solid peptides by dipolar-mediated 13C/15 N correlation solid-state NMR. J Am Chem Soc 120:7113–7114

Hong M, Su Y (2011) Structure and dynamics of cationic membrane peptides and proteins: insights from solid-state NMR. Protein Sci 20:641–655

Hu J, Asbury T, Achuthan S, Li C, Bertram R et al (2007) Backbone structure of the amantadine-blocked trans-membrane domain M2 proton channel from Influenza A virus. Biophys J 92:4335–4343

Hu KN, Yau WM, Tycko R (2010) Detection of a transient intermediate in a rapid protein folding process by solid-state nuclear magnetic resonance. J Am Chem Soc 132:24–25

Hu FH, Luo WB, Cady SD, Hong M (2011) Conformational plasticity of the influenza A M2 transmembrane helix in lipid bilayers under varying pH, drug binding, and membrane thickness. Biochim Biophys Acta 1808:415–423

Huang L, Nishinari K (2001) Interaction between poly(ethylene glycol) and water as studied by differential scanning calorimetry. J Polym Sci B Polym Phys 39:496–506

Kyrychenko A, Dyubko TS (2008) Molecular dynamics simulations of microstructure and mixing dynamics of cryoprotective solvents in water and in the presence of a lipid membrane. Biophys Chem 136:23–31

Labbe C, Crowe LM, Crowe JH (1997) Stability of the lipid component of trout sperm plasma membrane during freeze-thawing. Cryobiology 34:176–182

Lane LB (1925) Freezing points of glycerol and its aqueous solutions. Ind Eng Chem 17:924

Lange A, Giller K, Hornig S, Martin-Eauclaire MF, Pongs O et al (2006) Toxin-induced conformational changes in a potassium channel revealed by solid-state NMR. Nature 440:959–962

Linden AH, Franks WT, Akbey U, Lange S, van Rossum BJ et al (2011) Cryogenic temperature effects and resolution upon slow cooling of protein preparations in solid state NMR. J Biomol NMR 51:283–292

Long SB, Tao X, Campbell EB, MacKinnon R (2007) Atomic structure of a voltage-dependent k + channel in a lipid membrane-like environment. Nature 450:376–383

Loquet A, Sgourakis NG, Gupta R, Giller K, Riedel D et al (2012) Atomic model of the type III secretion system needle. Nature 486:276–279

Luo W, Hong M (2010) Conformational changes of an ion channel membrane protein detected through water-protein interactions using solid-state NMR spectroscopy. J Am Chem Soc 132:2378–2384

Maly T, Debelouchina GT, Bajaj VS, Hu KN, Joo CG et al (2008) Dynamic nuclear polarization at high magnetic fields. J Chem Phys 128:052211

Miller DP, dePablo JJ, Corti H (1997) Thermophysical properties of trehalose and its concentrated aqueous solutions. Pharm Res 14:578–590

Munowitz MG, Griffin RG, Bodenhausen G, Huang TH (1981) Two-dimensional rotational spin-echo NMR in solids: correlation of chemical shift and dipolar interactions. J Am Chem Soc 103:2529–2533

Murata KI, Tanaka H (2012) Liquid-liquid transition without macroscopic phase separation in a water-glycerol mixture. Nat Mater 11:436–443

Ni QZ, Daviso E, Can TV, Markhasin E, Jawla SK et al (2013) High frequency dynamic nuclear polarization. Acc Chem Res 46:1933–1941

Nomura K, Lintuluoto M, Morigaki K (2011) Hydration and temperature dependence of 13C and 1H NMR spectra of the DMPC phospholipid membrane and complete resonance assignment of its crystalline state. J Phys Chem B 115:14991–15001

Petsko GA (1975) Protein crystallography at sub-zero temperatures: cryo-protective mother liquors for protein crystals. J Mol Biol 96:381–392

Rasmussen DH, MacKenzi AP (1968) Phase diagram for the system water-dimethylsulphoxide. Nature 220:1315–1317

Rasmussen SG, DeVree BT, Zou Y, Kruse AC, Chung KY et al (2011) Crystal structure of the β2 adrenergic receptor-Gs protein complex. Nature 477:549–555

Renault M, Pawsey S, Bos MP, Koers EJ, Nand D et al (2012) Solid-state NMR spectroscopy on cellular preparations enhanced by dynamic nuclear polarization. Angew Chem Int Ed Engl 51:2998–3001

Rienstra CM, Tucker-Kellogg L, Jaroniec CP, Hohwy M, Reif B et al (2002) De novo determination of peptide structure with solid-state magic-angle spinning NMR spectroscopy. Proc Natl Acad Sci USA 99:10260–10265

Rosenbaum DM, Zhang C, Lyons JA, Holl R, Aragao D et al (2011) Structure and function of an irreversible agonist-beta(2) adrenoceptor complex. Nature 469:236–240

Siemer AB, Huang KY, McDermott AE (2012) Protein linewidth and solvent dynamics in frozen solution NMR. Plos One 7:e47242

Storey BT, Noiles EE, Thompson KA (1998) Comparison of glycerol, other polyols, trehalose, and raffinose to provide a defined cryoprotectant medium for mouse sperm cryopreservation. Cryobiology 37:46–58

Stouffer AL, Nanda V, Lear JD, DeGrado WF (2005) Sequence determinants of a transmembrane proton channel: an inverse relationship between stability and function. J Mol Biol 347:169–179

Su YC, Hong M (2011) Conformational disorder of membrane peptides investigated from solid-state NMR line widths and line shapes. J Phys Chem B 115:10758–10767

Su Y, Waring AJ, Ruchala P, Hong M (2010) Membrane-bound dynamic structure of an arginine-rich cell-penetrating peptide, the protein transduction domain of HIV TAT, from solid-state NMR. Biochemistry 49:6009–6020

Tang M, Hong M (2009) Structure and mechanism of beta-hairpin antimicrobial peptides in lipid bilayers from solid-state NMR spectroscopy. Mol BioSyst 5:317–322

Tang M, Waring AJ, Hong M (2007) Trehalose-protected lipid membranes for determining membrane protein structure and insertion. J Magn Reson 184:222–227

Tang M, Comellas G, Rienstra CM (2013) Advanced solid-state NMR approaches for structure determination of membrane proteins and amyloid fibrils. Acc Chem Res 46:2080–2088

Tivol WF, Briegel A, Jensen GJ (2008) An improved cryogen for plunge freezing. Microsc Microanal 14:375–379

Tycko R (2011) Solid-state NMR studies of amyloid fibril structure. Annu Rev Phys Chem 62:279–299

Tycko R (2013) NMR at low and ultra low temperatures. Acc Chem Res 46:1923–1932

Wang C, Wu H, Katritch V, Han GW, Huang XP et al (2013a) Structure of the human smoothened receptor bound to an antitumour agent. Nature 497:338–343

Wang T, Park YB, Caporini MA, Rosay M, Zhong LH et al (2013b) Sensitivity-enhanced solid-state NMR detection of expansin's target in plant cell walls. Proc Natl Acad Sci USA 110:16444–16449

Wasmer C, Lange A, Van Melckebeke H, Siemer AB, Riek R et al (2008) Amyloid fibrils of the HET-s(218-289) prion form a beta solenoid with a triangular hydrophobic core. Science 319:1523–1526

Yu ZW, Quinn PJ (1998) The modulation of membrane structure and stability by dimethyl sulphoxide (Review). Mol Membr Biol 15:59–68

Yu ZW, Quinn PJ (2000) The effect of dimethyl sulphoxide on the structure and phase behaviour of palmitoleoylphosphatidylethanolamine. Biochim Biophys Acta 1509:440–450